AIP | Applied Physics Letters

Coherent elastic waves in a one-dimensional polymer hypersonic crystal

P. M. Walker, J. S. Sharp, A. V. Akimov, and A. J. Kent

Citation: Applied Physics Letters **97**, 073106 (2010); doi: 10.1063/1.3479929
View online: http://dx.doi.org/10.1063/1.3479929
View Table of Contents: http://scitation.aip.org/content/aip/journal/apl/97/7?ver=pdfcov
Published by the AIP Publishing

Coherent elastic waves in a one-dimensional polymer hypersonic crystal

P. M. Walker, J. S. Sharp, A. V. Akimov, and A. J. Kent[a)]
School of Physics and Astronomy, University of Nottingham, University Park, Nottingham NG7 2RD, United Kingdom

(Received 24 June 2010; accepted 26 July 2010; published online 17 August 2010)

Using the methods of picosecond acoustics, we inject high amplitude hypersonic wavepackets into a polymer superlattice and optically detect the propagating coherent elastic waves. The spectrum of the optically detected signal shows the elastic modes typical for folded phonon dispersion curves. The experimental results and related modeling show the feasibility of using polymer one-dimensional hypersonic crystals as acoustic devices in the gigahertz frequency range. © *2010 American Institute of Physics*. [doi:10.1063/1.3479929]

Artificial structures with periodic acoustic impedance, known as phononic crystals, have been intensively studied and are already widely used in traditional kilohertz acoustics and megahertz ultrasonics for sound isolation and other applications.[1–5] Revolutionary "sound ideas" are widely discussed nowadays by introducing *hypersonic crystals* which are phononic crystals with submicrometer and nanometer period.[6] The specific acoustic properties of hypersonic crystals relate to dispersion folding and the existence of band gaps in the elastic spectrum at frequencies in the range 10^9-10^{12} Hz.

During the past decade researchers have performed a number of coherent acoustic experiments with one-, two-, and three-dimensional hypersonic crystals.[7–15] The next challenging step toward embedding the hypersonic crystals into integrated high-frequency acoustic circuits is a search for materials from which the required nanostructures could be fabricated with realistic technologies. A family of materials which could be ideal for this is polymers. Basic material properties such as elastic constants and sound velocities are known for a number of polymeric materials. The noncoherent acoustic properties of a number of polymer-based hypersonic crystals and lamellar diblock copolymers have been studied using conventional Brillouin scattering techniques and phononic band gaps in the gigahertz (GHz) frequency range have been observed.[16–18] These studies together with picosecond acoustic experiments performed on single polymer layers[19,20] and sub-GHz experiments in polymer containing multilayered structures[21] provide a strong reason for performing coherent acoustic experiments in polymer hypersonic crystals.

In the present work we explore the use of the picosecond acoustic technique to study the propagation of sound with a frequency of up to 20 GHz in a polymer superlattice, which is a classic example of a one-dimensional hypersonic crystal. We show that a high amplitude acoustic wavepacket, injected into a polymer nanostructure, does not lose its coherence during a time of the order a nanosecond. The acoustic spectrum of the propagating hypersonic wavepacket clearly shows the effect of phonon dispersion folding, which indicates the high quality of the structures with regard to both the periodicity and the interfaces formed between the polymer layers.

The polymer superlattice used consisted of five periods of polyvinylpyrrolidone (PVP), density=1230 kg m^{-3}, and polystyrene (PS), density=1050 kg m^{-3}, layers fabricated on a 110 micron thick (100) Si substrate crystalline silicon (Si) substrate, with PVP as the layer directly in contact with the Si. The layers were spin coated from 4 wt % solutions of PS and PVP in toluene and acetonitrile/ethanol (50/50), respectively. A drop of the corresponding solution was placed on the substrate and rotated at 4500 rpm. This procedure results in the production of uniform polymer films with thickness values that can be controlled to within $+/-1-2$ nm.[22] The thickness and refractive index values were measured using both a single wavelength nulling ellipsometer and a Woollam M2000V spectroscopic ellipsometer. Thickness values of $d_{pvp}=218+/-1$ nm and $d_{ps}=199+/-2$ nm were obtained and refractive index values of $n_{pvp}=1.543+/-0.001$ and $n_{ps}=1.628+/-0.001$ were measured at a wavelength of $\lambda=400$ nm for the PVP and PS layers, respectively, ($n_{pvp}=1.5145+/-0.001$ and $n_{ps}=1.5789+/-0.001$ at $\lambda=880$ nm). These values are consistent with the range of refractive indices obtained for different polymers.[23]

The hypersonic wavepacket is injected into the polymer structure from the (001) Si substrate by means of the picosecond acoustic technique.[24] The corresponding experimental scheme is shown in the inset of Fig. 1(a). An Al film with a thickness ~100 nm was deposited on the side of the Si substrate opposite to the polymer. The film was excited by 60 fs pump pulses generated by a titanium sapphire laser (wavelength 800 nm) followed by a regenerative amplifier with repetition rate of 5 kHz. The diameter of the excitation spot was 200 μm and the maximum energy density in the pulse on the Al film was 6 mJ/cm^2. As a result of the optical excitation, the Al film expands due to the thermoelastic effect and a bipolar strain pulse with an amplitude of $\sim 10^{-3}$ is injected into the Si substrate. The strain pulse propagates through the Si substrate and reaches the Si/PVP interface of the polymer nanostructure in a time $t_0=d_{Si}/s_{Si}=13.0$ ns ($d_{Si}=110$ μm and $s_{Si}=8430$ m/s are the thickness of Si substrate and LA sound velocity in Si, respectively). The strain pulse is partly reflected back to the Si substrate and partly transmitted into the polymer superlattice.

Detection of the hypersound wavepackets in the polymer superlattice is realized by probing the optical reflectivity R of the structure with a pulse originating from the same laser system which excites the strain pulses [inset in Fig. 1(a)].

a)Electronic mail: anthony.kent@nottingham.ac.uk.

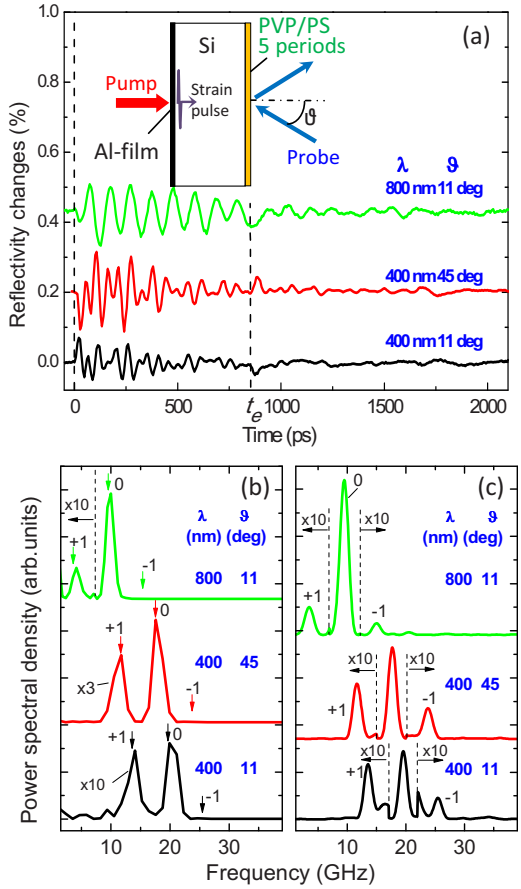

FIG. 1. (Color online) (a) The temporal evolution of the measured reflectivity signal of the probe pulse, with wavelength λ and incident angle θ, when the acoustic wavepacket is propagating through the PVP/PS superlattice. The values $t=0$ and $t=t_e$ marked by dashed vertical lines correspond, respectively, to the time between probe and pump pulses when the picosecond strain pulse is injected into a superlattice from the Si substrate and when the strain pulse reaches the superlattice/air interface. The inset shows the experimental scheme. (b) The fast Fourier transforms of the signals shown in (a) for corresponding λ and θ. (c) The calculated spectra of the displacement in the superlattice caused by the injected acoustic wavepacket for wave vectors $q_{\lambda,\vartheta}=2k_{\perp}$ which are active in the optically probed signals for corresponding pairs of λ and θ.

The probe beam is passed through an optical delay line, thus allowing scanning of the time interval, t, between pump and probe pulses. The probe optical beam is incident on the surface of the superlattice opposite the pump excitation at an angle of incidence θ and the specularly reflected beam is measured by a photodetector. The interference of the probe beam reflections from the interfaces and the acoustic wavepacket propagating in the superlattice results in the temporal modulation of R, and the oscillations $R(t)$ as a function of t can be detected.[25] In the case of homogeneous semi-infinite media these oscillations have a single Brillouin frequency as follows:

$$f = 2s\lambda^{-1}\sqrt{n^2 - \sin^2\vartheta}, \tag{1}$$

where s is the sound velocity, λ is the wavelength of the probing beam in air, and n is the refractive index of the medium. In the case of a film with a finite thickness, $R(t)$ can be analyzed using well developed methods.[26] Using this standard probing technique we have obtain the values $s_{ps}=2230\pm40$ m/s and $s_{pvp}=2800\pm200$ m/s in the single PS

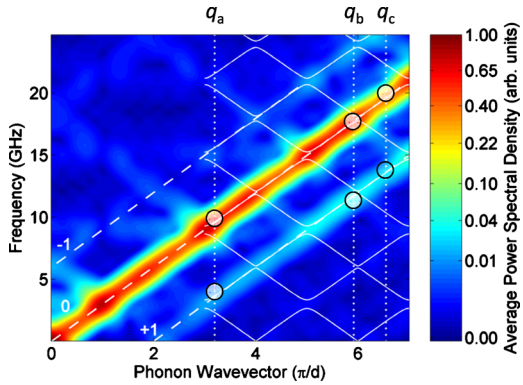

FIG. 2. (Color online) The solid lines are the calculated dispersion relations $f(q)$ in the direction perpendicular to the plane of the polymer superlattice (the period of the SL $d=417$ nm). The crossings of the solid and dotted vertical lines correspond to the momentum conservation for phonon–photon interaction giving the frequency components which are detected optically in the performed experiments for corresponding pairs λ and θ: q_a, q_b, and q_c correspond to the pairs (λ=800 nm, $\theta=11°$), (λ=400 nm, $\theta=45°$), and (λ=400 nm, $\theta=11°$), respectively. The dashed diagonal lines indicate the main "0" and sideband "+1" and "−1" spectral components which arise from the folding of the acoustic dispersion due to the superlattice. The grayscale (color scheme) shows the intensity of the acoustic modes for the displacement calculated in the system. The circular points indicate the frequencies of the modes detected in the experiment [taken from Fig. 1(b)].

and PVP layers, respectively, which are in a good agreement with previously measured values.[19,27]

Figure 1(a) shows the reflectivity signals $\Delta R(t)/R_0$, where $\Delta R(t)=R(t)-R_0$, where R_0 is the stationary reflectivity in the absence of the strain pulse, measured in the polymer superlattice described above for two various probe wavelengths λ and incidence angles θ. The oscillatory behavior of $\Delta R(t)/R_0$ is clearly observed. The oscillations have longer period for λ=800 nm than for λ=400 nm which is in qualitative agreement with Eq. (1). The vertical dashed line in Fig. 1(a) indicates the time $t_e=D/\bar{s}$ when the strain pulse has traversed the whole superlattice and reached the edge of the sample at the PS/air interface. Here $D=2.1$ μm is the total thickness and $\bar{s}=2500$ m/s is an average sound velocity in the polymer superlattice. It is seen that for $t<t_e$ the oscillations are not damped completely and the decay for λ=800 nm is less rapid than for λ=400 nm.

Figure 1(b) shows the fast Fourier transforms obtained from the measured data $\Delta R(t)/R_0$. Each spectrum clearly shows two peaks with the frequencies depending on the combination of λ and θ. The spectral peaks labeled as "0" are centered at frequencies f_0 which are consistent with those expected from Eq. (1) when average values $\bar{s}=2500$ m/s and $\bar{n}=1.583$ are used. Another peak labeled "+1" has a frequency 6 GHz lower and is not expected to be present in a homogeneous medium. The amplitude of the "0" and "+1" peaks are comparable for λ=400 nm but at λ=800 nm the "0" peak dominates the spectrum.

The observation of the "+1" spectral peak in the Fourier spectrum of the measured signal is the main experimental result of the present work. We associate this peak with the properties of the one-dimensional hypersonic crystal; specifically constructive interference of the partial reflections of the strain wavepacket at the interfaces of the periodic structure. To show this we present in Fig. 2 the calculated acoustic dispersion curves for longitudinal (LA) modes in the extended Brillouin zone. The color scheme in Fig. 2 shows the

calculated spectral density of displacement for the acoustic modes in the system by performing Fourier transforms in the time window 0–790 ps, which corresponds to the time interval considered for the experimental data. It is seen that the "0" mode has a maximum amplitude and the amplitudes of the side modes are smaller.

The relative intensities of the measured peaks $P_{f,i}$ [Fig. 1(b)] may be compared with the calculated spectral densities of the displacement (Fig. 2), under the assumption that the acousto-optical coupling is independent of the acoustic frequency at the particular λ and θ. The corresponding calculated spectra are shown in Fig. 1(c) for the pairs λ and θ used in the experiment. The relative amplitudes of the "0" and "+1" peaks at a given wavelength which, when compared with the experimental data presented in Fig. 1(b), gives a good agreement for $\lambda = 800$ nm. However, for the two other experimental conditions, the experimentally measured "0" and "+1" peaks have similar intensities, while in the calculated spectra the "0" peak is significantly stronger. The reason for such disagreement is probably due to the rapid high-frequency cutoff of the acoustic wavepacket spectrum in the polymer superlattice. Indeed, from the comparison of the intensity $P_{f,0}$ for the "0" peak measured for various pairs of λ and θ [Fig. 1(b)] we see that the $P_{f,0}$ decreases strongly with the increase in f. The likely reason for a high-frequency cutoff is a strong frequency dependence of attenuation $\alpha(f) = A_{ps} f^2$ ($A_{ps} = 2.5 \times 10^{-15}$ m^{-1} Hz^{-2} for the PS film) in the polymer structure.[19] Thus, in PS, the mean free path $\alpha^{-1}(f) = 4 \times 10^{-6}$ m for $f = 10$ GHz and 10^{-6} m for $f = 20$ GHz. The latter value is half the total thickness of the structure and so the 20 GHz component of the wavepacket will be more strongly damped than the component at 10 GHz. In agreement with this estimate, the experimentally measured signals [Fig. 1(a)] decay faster for $\lambda = 400$ nm than for $\lambda = 800$ nm. The high frequency cutoff also accounts for some suppression of the "−1" peak relative to the "+1."

In summary, our experiments show that the periodic polymer multilayer structure possesses acoustic properties typical for one-dimensional hypersonic crystals. This opens the way for fabrication of complex polymer hypersonic nanostructures for sound manipulation at frequencies higher than 10 GHz. A good agreement between the experiment and theory shows that propagation of hypersound through the interfaces between polymer layers can be modeled by the standard acoustic mismatch approach but the frequency dependence of attenuation should be taken into account on the submicrometer scale.

We are thankful to Boris Glavin for helpful discussion. We acknowledge EPSRC for financial support.

[1] R. Martínez-Sala, J. Sancho, J. V. Sánchez-Pérez, J. Llinares, and F. Meseguer, Nature (London) **378**, 241 (1995).
[2] Z. Liu, X. Zhang, Y. Mao, Y. Y. Zhu, Z. Yang, C. T. Chan, and P. Sheng, Science **289**, 1734 (2000).
[3] S. Yang, J. H. Page, Z. Liu, M. L. Cowan, C. T. Chan, and P. Sheng, Phys. Rev. Lett. **93**, 024301 (2004).
[4] O. Holmgren, J. V. Knuuttila, T. Makkonen, K. Kokkonen, V. P. Plessky, W. Steichen, M. Solal, and M. M. Salomaa, Appl. Phys. Lett. **86**, 024101 (2005).
[5] A. Khelif, A. Choujaa, S. Benchabane, B. Djafari-Rouhani, and V. Laude, Appl. Phys. Lett. **84**, 4400 (2004).
[6] T. Gorishnyy, C. K. Ullal, M. Maldovan, G. Fytas, and E. L. Thomas, Phys. Rev. Lett. **94**, 115501 (2005).
[7] A. Yamamoto, T. Mishina, and Y. Masumoto, Phys. Rev. Lett. **73**, 740 (1994).
[8] A. Bartels, T. Dekorsy, H. Kurz, and K. Kohler, Phys. Rev. Lett. **82**, 1044 (1999).
[9] C.-K. Sun, J.-C. Liang, and X.-Y. Yu, Phys. Rev. Lett. **84**, 179 (2000).
[10] E. Makarona, B. Daly, J.-S. Im, H. Maris, A. Nurmikko, and J. Han, Appl. Phys. Lett. **81**, 2791 (2002).
[11] M. Trigo, T. Eckhause, M. A. Reason, R. S. Goldman, and R. Merlin, Phys. Rev. Lett. **97**, 124301 (2006).
[12] A. Huynh, N. D. Lanzillotti-Kimura1, B. Jusserand, B. Perrin, A. Fainstein, M. F. Pascual-Winter, E. Peronne, and A. Lemaître, Phys. Rev. Lett. **97**, 115502 (2006).
[13] R. P. Beardsley, A. V. Akimov, M. Henini, and A. J. Kent, Phys. Rev. Lett. **104**, 085501 (2010).
[14] D. M. Profunser, O. B. Wright, and O. Matsuda, Phys. Rev. Lett. **97**, 055502 (2006).
[15] A. S. Salasyuk, A. V. Scherbakov, D. R. Yakovlev, A. V. Akimov, A. A. Kaplyanskii, S. F. Kaplan, S. A. Grudinkin, A. V. Nashchekin, A. B. Pevtsov, V. G. Golubev, T. Berstermann, C. Brüggemann, M. Bombeck, and M. Bayer, Nano Lett. **10**, 1319 (2010).
[16] W. Cheng, J. J. Wang, U. Jonas, G. Fytas, and N. Stefanou, Nature Mater. **5**, 830 (2006).
[17] N. Gomopoulos, D. Maschke, C. Y. Koh, E. L. Thomas, W. Tremel, H.-J. Butt, and G. Fytas, Nano Lett. **10**, 980 (2010).
[18] A. M. Urbas, E. L. Thomas, H. Kriegs, G. Fytas, R. S. Penciu, and L. N. Economou, Phys. Rev. Lett. **90**, 108302 (2003).
[19] C. J. Morath and H. J. Maris, Phys. Rev. B **54**, 203 (1996).
[20] Y. C. Lee, K. C. Bretza, F. W. Wise, and W. Sachse, Appl. Phys. Lett. **69**, 1692 (1996).
[21] G. Saini, T. Pezeril, D. H. Torchinsky, J. Yoon, S. E. Kooi, E. L. Thomas, and K. A. Nelson, J. Mater. Res. **22**, 719 (2007).
[22] J. S. Sharp and J. A. Forrest, Phys. Rev. Lett. **91**, 235701 (2003).
[23] *Polymer Handbook*, edited by J. Brandrup, E. H. Immergut, and E. A. Grulke (Wiley, New Jersey, 1999).
[24] C. Thomsen, H. T. Grahn, H. J. Maris, and J. Tauc, Phys. Rev. B **34**, 4129 (1986).
[25] H. N. Lin, R. J. Stoner, H. J. Maris, and J. Tauc, J. Appl. Phys. **69**, 3816 (1991).
[26] O. B. Wright, J. Appl. Phys. **71**, 1617 (1992).
[27] W. Cheng, R. Sainidou, P. Burgardt, N. Stefanou, A. Kiyanova, M. Efremov, G. Fytas, and P. F. Nealey, Macromolecules **40**, 7283 (2007).